Laser Photoluminescence Spectra of $^{24}Mg_2$ and $^{26}Mg_2$ in Solid Argon at 12 K

John C. Miller and Lester Andrews*

Contribution from the Chemistry Department, University of Virginia, Charlottesville, Virginia 22901. Received October 12, 1977

Abstract: Magnesium-24 and -26 atoms were codeposited with argon at 12 K and the Mg$_2$ van der Waals dimer, formed from atomic diffusion in the freezing matrix, has been examined. Electronic absorption and emission spectra were observed for Mg$_2$ and the constants T_e = 26 226 cm^{-1}, ω_e' = 179 ± 1 cm^{-1}, $\omega_e x_e'$ = 1.2 ± 0.2 cm^{-1}, ω_e'' = 90.8 ± 0.5 cm^{-1}, $\omega_e x_e''$ = 0.60 ± 0.15 cm^{-1} determined for the $^{24}Mg_2$ $^1\Sigma_u^+$ (^{1}S + ^{1}P) ← $^1\Sigma_g^+$ (^{1}S + ^{1}S) transition. These constants are consistent with a simple molecular orbital picture which predicts a van der Waals ground state and a chemically bound excited state. A second much weaker structured absorption with average spacings of 194 cm^{-1} was observed, and its assignment is considered. Matrix cage effects and vibrational relaxation are discussed.

Introduction

Recently, a great deal of experimental and theoretical work has focused on the group 2A and 2B metal dimers.[1-18] This novel class of compounds is characterized by a chemically unbound ground state due to an equal number of electrons in bonding and antibonding orbitals; the only ground-state attraction is of a van der Waals nature. Low-lying excited states are, however, expected to be bound following excitation of an antibonding electron to a bonding orbital. These characteristics make van der Waals dimers attractive candidates as the active medium for new lasers as well as very interesting chemical compounds in their own right.

Gas-phase electronic absorption and emission studies have identified Mg$_2$ and Ca$_2$ and provided detailed spectroscopic constants.[1-5] Another quite fruitful approach, however, has been the matrix-isolation technique where these relatively unstable molecules can be generated and trapped within a matrix of frozen inert gas at low temperatures. The group 2A dimers Be$_2$,[6] Mg$_2$,[7-9] Ca$_2$,[9-12] and Sr$_2$[9] as well as the group 2B compounds Zn$_2$[13] and Cd$_2$[13,14] have been studied in this way and their absorption spectra have both identified the molecules and characterized their bound excited states. Also, the heteronuclear molecules CaMg, SrMg, BaMg, and SrCa[9] and ZnCd, MgCd, MgZn, MgHg, CdHg, and ZnHg[15] have been observed in solid argon. However, of more interest, are the properties of the van der Waals ground state derived from emission studies. To date, only Ca$_2$ emission has been reported in matrices.[12,16,17]

Mg$_2$ is considered a prototype for these alkaline earth dimers as it is well characterized in the gas phase[1] and is small enough to be amenable to ab initio calculations.[18]

This works reports absorption and emission studies of Mg$_2$ in frozen argon. Although the absorption has been studied extensively,[7-9] no isotope work has been reported and the matrix emission spectrum has not been previously observed.

Experimental Section

The experimental apparatus has been described elsewhere.[9,16] Briefly, ^{24}Mg (99.99%, Dow Chemical Co.) or ^{26}Mg (>95%, Oak Ridge National Laboratory) was placed in a resistance heated Knudsen cell and outgassed. Matrices were prepared by codepositing argon (99.99%, Air Products) at 2–3 mmol/h with the effusing beam of metal atoms (oven temperature 300–350 °C) on a sapphire window at 10 K for absorption or a polished copper block at 12 K for emission. It is interesting to note that a sliding door in front of the Knudsen cell proved ineffective for containing magnesium atoms, presumably owing to a low sticking coefficient. The most dilute experiments were obtained by depositing metal atoms with this door *closed.*

Absorption spectra were recorded on a Cary 17 spectrophotometer from 500 to 200 nm both during and after deposition. The dimer ab-

sorptions of interest were then recorded on an expanded wavelength scale at 0.1 or 0.2 nm/s. Calibration was provided by superimposing Hg emission lines from a low-pressure penlight. Absorption band measurements are accurate to ±0.1 nm.

In emission studies, excitation was provided by the 351.1/363.8 nm or the 350.7/356.4 nm lines from Coherent Radiation argon ion or krypton ion lasers, respectively. A dielectric filter was used to remove plasma emission lines; typically the laser power was 40–60 mW at the sample. In some experiments the individual laser lines were separated by passing them through two coupled Spex "mini-mate" monochromators. The luminescence was focused on the slit of a Spex 1401 double monochromator and detected by a cooled RCA C31034 phototube. Typical spectral band width was ~4 cm^{-1} (100-μ slits). Calibration was accomplished by scanning over the laser line and then through the emission. In most experiments additional Hg emission lines were also superimposed on the spectrum. Emission band measurements are accurate to ±5 cm^{-1}.

Results

Absorption. Although the ^{24}Mg$_2$ adsorption spectrum has been studied previously,[7-9] it was necessary to more carefully calibrate the spectrum for comparison with that of ^{26}Mg$_2$ and with the emission. Figure 1 shows the absorption spectra from 380 to 354 nm of (a) ^{24}Mg$_2$ and (b) ^{26}Mg$_2$ in solid argon at 10 K. The structured bands exhibit ten member progressions with average spacings of 169 cm^{-1} for ^{24}Mg$_2$ and 161 cm^{-1} for ^{26}Mg$_2$. The vibronic band positions are listed in Table I. A much weaker band system is observed around 445 nm with four vibronic bands spaced 194 and 185 cm^{-1} for ^{24}Mg$_2$ and ^{26}Mg$_2$, respectively. The intensity of this system is on the order of 2% of the higher energy absorption. This band is shown in Figure 2 and also tabulated in Table I. Each vibronic band is split into three components; only the center peak position is listed in the table.

Emission. Upon UV laser excitation, a strong, structured emission band was observed peaking around 25 600 cm^{-1} for ^{24}Mg$_2$. This band system, shown in Figure 3(a), exhibits a strong, sharp, 18-member vibronic progression with spacings ranging from about 90 cm^{-1} for the higher energy bands to about 80 cm^{-1} for the lower energy bands. Each sharp peak is accompanied by a weaker, somewhat broader sideband about 35 cm^{-1} to the red. The energies and spacings for the sharp bands are listed in Table II. The relative intensity and resolution of the strong and weak progressions did not change on temperature cycling (12–25–12 K). At 15 and 20 K a reversible transfer of intensity to the sideband was noted along with a general loss of resolution. At 25 K no resolvable structure was observed.
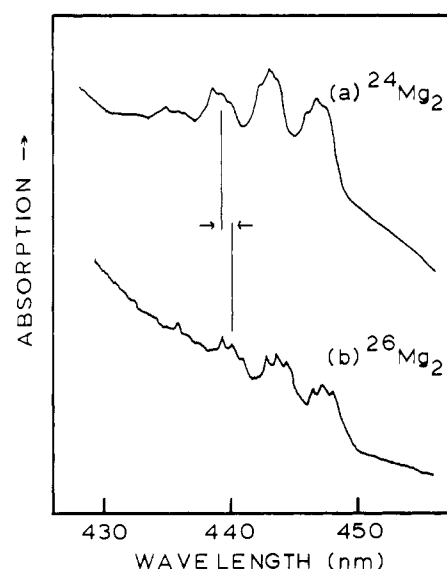
Although the 356.4-nm krypton ion line falls between the 11 ← 0 and 12 ← 0 absorptions and the 363.8-nm argon ion line is very near resonance with the 8 ← 0 absorption, both

Table I. Absorption Bands for $^{24}Mg_2$ and $^{26}Mg_2$ in Argon at 10 K

	$^{24}Mg_2$			$^{26}Mg_2$			Isotope
v'	λ, nm	$\bar{\nu}$, cm^{-1}	Δ cm^{-1}	λ, nm	$\bar{\nu}$, cm^{-1}	Δ, cm^{-1}	shift, cm^{-1}
0							
1							
2	376.7	26 546		377.1	26 518		28
3	374.0	26 709	163	374.7	26 688	170	21
4	371.9	26 889	180	372.3	26 860	172	29
5	369.6	27 056	167	370.1	27 020	160	36
6	367.4	27 218	162	368.0	27 174	154	44
7	365.2	27 382	164	365.9	27 330	156	52
8	362.9	27 556	174	363.7	27 495	165	61
9	360.6	27 731	175	361.5	27 662	167	69
10	358.5	27 894	163	359.5	27 816	154	78
11	356.3	28 066	172	357.5	27 972	156	94
12	354.2	28 233	167	355.5	28 130	158	103
			Av 169			Av 161	
2	447.0	22 371		447.3	22 356		15
3	443.2	22 563	192	443.6	22 543	187	20
4	439.4	22 758	195	440.1	22 722	179	36
5	435.7	22 954	194	436.5	22 910	188	42
			Av 194			Av 185	
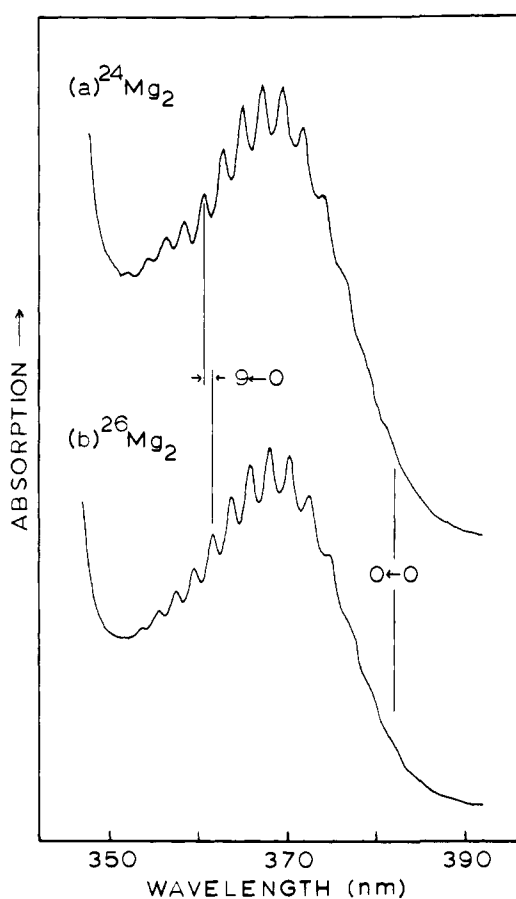
Figure 1. The intense structured absorption band of (a) $^{24}Mg_2$ and (b) $^{26}Mg_2$ recorded on a Cary 17 at 0.1 nm/s. The electronic origin is noted and the isotope shift of the 9 ← 0 vibronic bands is portrayed.

Figure 2. The weak structured absorption band of (a) $^{24}Mg_2$ and (b) $^{26}Mg_2$ recorded on the 0–0.2 absorbance scale.

excitations produced identical relative intensities and resolution in the emission spectra. This is in contrast with the Ca_2 emission[12,16] where off-resonance excitation gave either poorly resolved or continuum emission owing presumably to multiple trapping sites. Use of a monochromator to resolve the individual argon and krypton laser lines resulted in identical spectra for all four excitations. The higher energy lines from each laser, which also fall within an aggregate absorption,[8,9]

produced the characteristic Mg_2 spectrum, but much weaker.

The corresponding emission from $^{26}Mg_2$ is shown in Figure 3(b) and the peak positions listed in Table II. The 20-member progression, with spacings ranging from 86 to 75 cm^{-1}, is completely analogous to the $^{24}Mg_2$ spectrum with each peak isotope shifted.

An attempt was made to observe laser excited emission from Mg_2 in solid krypton; however, the argon ion and krypton ion ultraviolet laser lines miss the absorption band entirely,[9] and no dimer emission was observed.

Discussion

Vibronic Analysis–Emission. The emission data will be considered first as the bands can be measured more accurately and the analysis is more straightforward. The sharper, more intense bands in Figure 3 are assigned to the zero-phonon lines, and the broader sidebands 35 cm^{-1} to lower energy are attributed to phonon wings arising from coupling of the ground state Mg_2 vibration to the argon lattice vibrations. This interpretation is consistent with the constant relative intensities
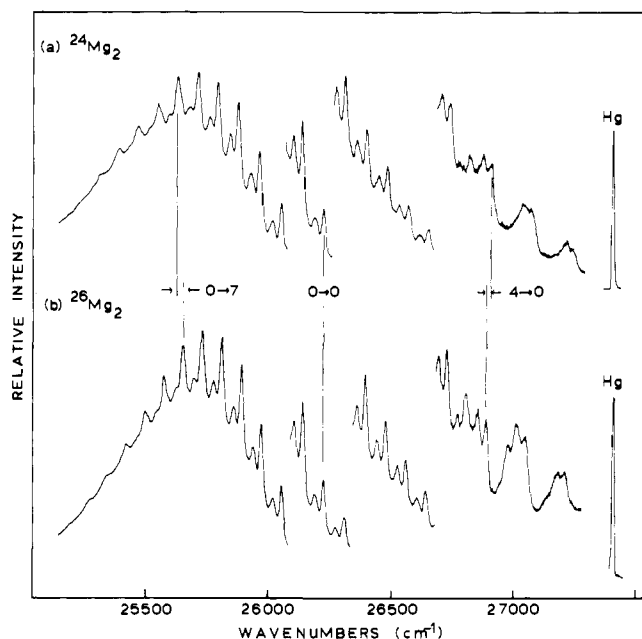
Figure 3. Photoluminescence spectrum of (a) $^{24}Mg_2$ and (b) $^{26}Mg_2$. The 0–0 band is labeled and the isotope shifts in the $0 \rightarrow 7$ and $4 \rightarrow 0$ transitions, are displayed. A mercury calibration line is included in the spectra.

Table II. Emission Bands and Spacings for $^{24}Mg_2$ and $^{26}Mg_2$ in Argon at 12 K

$v'-v''$	$^{24}Mg_2$ $\bar{\nu}$, cm⁻¹	$^{24}Mg_2$ Δ, cm⁻¹	$^{26}Mg_2$ $\bar{\nu}$, cm⁻¹	$^{26}Mg_2$ Δ, cm⁻¹	Isotope shift
6–0	27 249	} 170	27 219	} 160	−30
6–1					
5–0	27 079	} 165	27 059 }	75	−20
5–1			26 984 }	} 165	
4–0	26 914 }	86	26 894 }	86	−20
4–1	26 828 }	} 166	26 808 }	} 163	
3–0	26 748 }	90	26 731 }	80	−17
3–1	26 658 }	} 172	26 644 }	} 167	
2–0	26 576 }	90	26 564 }	86	−12
2–1	26 486 }	} 175	26 478 }		
1–0	26 401 }	90	26 396 }	} 168	−5
1–1	26 311 }	} 175	26 311 }		
0–0	26 226		26 226	} 170	0
0–1	26 136	90	26 141	85	5
0–2	26 048	88	26 056	85	8
0–3	25 961	87	25 972	84	12
0–4	25 876	85	25 888	84	12
0–5	25 794	82	25 808	80	14
0–6	25 711	83	25 728	80	17
0–7	25 626	85	25 648	80	22
0–8	25 546	80	25 570	78	24
0–9	25 466	80	25 493	77	27
0–10	25 384	82	25 416	77	32
0–11			25 341	75	
			25 266	75	

of the two series on sample annealing and the reversible intensity shift to the broader series with increasing sample temperature.

The vibronic numbering of the emission progressions is based on the invariance of the 0–0 band to isotopic substitution and confirmed by a comparison of calculated and observed isotope shifts for other bands. This analysis is shown in Figure 4 where the absolute value of the isotopic shift is plotted against the vibronic quantum numbers for the excited state ($v' \rightarrow 0$ series) and the ground state ($0 \rightarrow v''$ series). The dotted lines indicate the calculated values based on a harmonic Mg–Mg vibration. The observed slopes of 3.2 and 5.5 cm⁻¹/quantum are slightly less than the calculated values of 3.6 and 7.0 cm⁻¹/quantum, respectively, as expected due to anharmonicity. When anharmonicity is included, the experimental points are fit to the calculated curves, within experimental error. The numbering is complicated by the overlapping of emission bands as the excited-state frequency is twice the ground-state frequency; e.g., the $1 \rightarrow 2$ band would be coincident with the $0 \rightarrow 0$ band. However, each successive "hot progression" should be weaker than the preceding one as vibrational quenching should increase as v' increases. Thus in Table II the bands have been assigned using the lowest v' and v'' numbering.

The ground state constants ω_e'' and $\omega_e x_e''$ were determined graphically in the usual manner. Figure 5 shows a plot of $G(v) - G(0))/v''$ vs. v'' from which the slope gives $-\omega_e x_e''$ and the intercept $\omega_e'' - \omega_e x_e''$. For $^{24}Mg_2$, $\omega_e'' = 90.8 \pm 0.5$ cm⁻¹ and $\omega_e x_e'' = 0.60 \pm 0.15$ cm⁻¹, and for $^{26}Mg_2$, $\omega_e'' = 86.9 \pm 0.3$ cm⁻¹ and $\omega_e x_e'' = 0.54 \pm 0.05$ cm⁻¹. The isotope shifts in ω_e'' of 3.9 cm⁻¹ and in $\omega_e x_e''$ of 0.06 cm⁻¹ compare well with the calculated values of 3.6 and 0.05 cm⁻¹, respectively.

The ground-state dissociation energy is of interest for a van der Waals molecule like Mg_2 as this value provides a measure of the strength of the attractive dispersion forces. An upper limit for the value of D_e'' can be obtained from the expression $D_e'' = (\omega_e'')^2/4\omega_e x_e''$ which gives $D_e'' = 3400 \pm 800$ cm⁻¹ for $^{24}Mg_2$ and 3500 ± 300 cm⁻¹ for $^{26}Mg_2$. A lower limit can be found by simply noting the energy of the highest observed discrete vibronic peak of the ground state. This lower limit is 842 cm⁻¹ for $^{24}Mg_2$ and 960 cm⁻¹ for $^{26}Mg_2$. Note that dis-

crete vibrational levels were observed for Mg_2 in solid argon above *double* the dissociation energy of gaseous Mg_2.

Using the lower and upper limits for D_e'' given above, the excited state dissociation energy, given by the expression

$$D' = E(^1P \leftarrow {}^1S) - E(0\text{–}0) + D''$$

can be estimated as 10 330 cm⁻¹ for a lower bound and 12 888 cm⁻¹ for an upper bound.

The presence of unrelaxed emission in the $v' \rightarrow 0$ series allows calculation of the excited state constants, although these are less accurate owing to having only six values. A plot similar to Figure 5 gives $\omega_e' = 179 \pm 1$ and 172 ± 1 cm⁻¹ and $\omega_e x_e' = 1.2 \pm 0.2$ and 0.1 ± 0.1 cm⁻¹ for $^{24}Mg_2$ and $^{26}Mg_2$, respectively. Again, the observed 7 cm⁻¹ isotope shift of ω_e' is in agreement with the calculated value of 7.0 cm⁻¹.

Vibronic Analysis–Absorption. Owing to the width of the absorption bands and the greater difficulty of measuring the peak maximum accurately, the analysis is less certain than for the emission data. A plot of isotope shift vs. quantum number, similar to Figure 4 for the emission, gives the numbering in Table I. The observed slope is, however, 7.5 cm⁻¹/quantum, which is slightly greater than the calculated value of 7.0, contrary to the effect expected from anharmonicity considerations. It must be realized that an optimistic estimate of the error in calibration and peak measurement is ±0.1 nm and that the displacement of one isotopic spectrum from that of the other by 0.1 nm leads to a change in the vibronic assignment by 1 quantum. Therefore the numbering in Table I must be considered correct to only ±1 quantum.

In addition, the energies of the $v' = 2\text{–}6 \leftarrow v'' = 0$ bands and the extrapolated 0–0 band do not agree with the corresponding band energies from the emission spectra. As the difference of about 35 cm⁻¹ is greater than experimental error and in view of the careful calibration described in the Experimental Section, a physical explanation must be found for this discrepancy. Furthermore, for the similar Ca_2 molecule, whose absorption[9] and emission[12,16] were measured on the same instruments, no such discrepancy was observed.

On first examination, the sharp emission bands and the much broader absorption bands would suggest that zero pho-
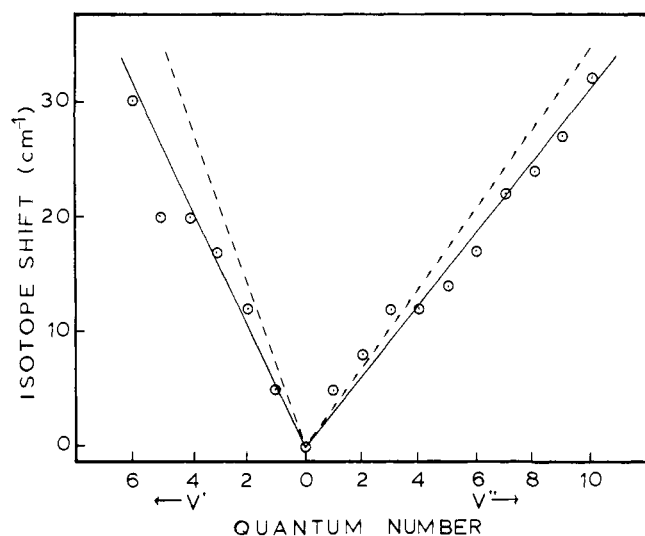
Figure 4. Plot of the absolute value of the isotope shift vs. the quantum number assignment for the unrelaxed and relaxed emission: experimental. —; harmonic calculation, - - - -.

Figure 5. Vibrational analysis of the structured emission of $^{24}Mg_2$ and $^{26}Mg_2$.

non lines are observed in the latter and only phonon side bands in the former which would lead to a discrepancy in the band energies. However, if this were the case, the absorption measurements would be *higher* in energy than the emission, contrary to what is observed. Furthermore, as the excited state is less polarizable and hence less interactive than the ground state, one would expect to observe zero phonon lines in absorption as well as emission. In principle, it is possible in rare gas solids for the absorption and emission to differ due to solvent reorientation around the excited state molecule because of a large change in size or polarizability between the upper and lower states.[19,20] This is certainly the case for a van der Waals molecule where the ground state is quite polarizable owing to the weak bonding. The excited state, however, is smaller and less polarizable because of the additional chemical bonding. For example, in the gas phase[1] the excited state r_e is 3.082 Å compared to 3.890 Å for the ground state of Mg_2. The comparable matrix change in r_e is about 0.5 Å as will be discussed later. Although this is a plausible explanation, it appears strange that no such discrepancy occurred for the very similar Ca_2 molecule.

The most likely explanation, however, lies in consideration of multiple trapping sites for Mg_2 in solid argon. If the absorption band maxima really reflect an average of several sites, slightly displaced in energy, with roughly equal populations and the narrow bandwidth laser excitation selects only one of these sites, then such a discrepancy would be expected. Argon is notorious for providing multiple sites and, indeed, for Ca_2, three such sites have been well characterized with tunable dye laser excitation.[17] Furthermore, the lower energy Mg_2 absorption in Figure 2 clearly shows triplet substructure and, in some spectra, the band under consideration also shows hints of fine structure. In summation, sites seem to provide the best explanation; however, a definitive answer must await either tunable excitation or the ability to excite Mg_2 in krypton or xenon matrices where phonon effects could be distinguished from site effects.

For the above reasons, and owing to the large scatter in the experimental spacings, no spectroscopic constants are given for the absorption data. The average spacings and isotope shifts are, however, consistent with those obtained from the emission spectrum.

The lower energy structured absorption around 440 nm is of interest as it has not been observed in other laboratories. The isotope study shows that this system is due to a magnesium-
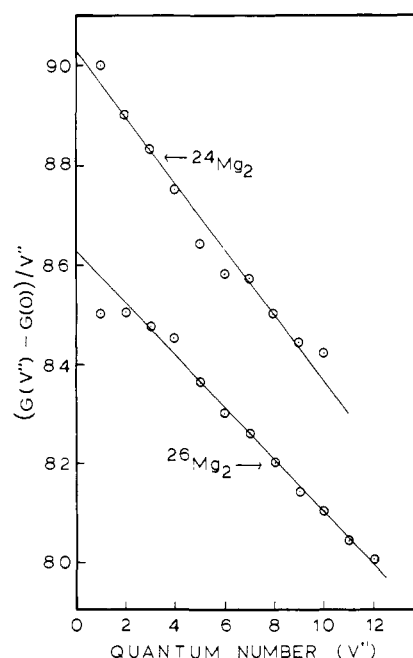
containing species, as suggested previously.[9] The average spacings of 194 and 185 cm^{-1} for the two isotopes and the shift of 9 cm^{-1} are reasonable for a diatomic magnesium species. Although the trimer assignment for this band cannot be ruled out, the Mg_3 species is considered less likely for two reasons. The growth pattern of the weaker 440-nm band appears to track with the stronger 367-nm dimer band. A straightforward MO picture for excited state Mg_3 using 3s and 3p orbitals on the central magnesium atom and 3s orbitals on the terminal atoms suggests weaker bonding than for excited state Mg_2 and a correspondingly lower symmetric stretching mode for Mg_3 than for Mg_2; the observed 194-cm^{-1} spacings are more appropriate for Mg_2 than Mg_3. The vibrational numbering in Table I is based on the isotope shifts and again is only considered accurate to ±1 quantum.

Electronic Assignment. Relatively straightforward molecular orbital theory is sufficient to describe the bonding and spectroscopy of the magnesium dimer. The ground-state valence configuration is, in the usual notation, $(\sigma_g 3s)^2 (\sigma_u 3s)^2$ leading to the designation $X^1\Sigma_g^+$ ($^1S + {}^1S$). As the σ_g orbital is bonding and the σ_u orbital is antibonding, the formal bond order is zero and a repulsive ground state is predicted. However, a shallow minimum in the potential well is produced by weak, attractive van der Waals forces. This description is entirely consistent with the lower state constants derived from the gas-phase absorption[1] and the matrix emission studies reported here.

The four possible low-lying singlet excited states, $^1\Pi_g$, $^1\Sigma_u^+$, $^1\Sigma_g^+$, and $^1\Pi_u$, correlating with $^1S + {}^1P$ isolated atoms result from excitation of either the σ_g or σ_u electron to either the $(\pi_u 3p)$ or the $(\sigma_g 3p)$ orbital. Only two of these configurations, $(\sigma_g 3s)^2 (\sigma_u 3s)^1 (\pi_u 3p)^1 - {}^1\Pi_g$ and $(\sigma_g 3s)^2 (\sigma_u 3s)^1 (\sigma_g 3p)^1 - {}^1\Sigma_u^+$, are strongly bound, and of these, only the $^1\Sigma_u^+$ state has the correct symmetry to couple with the gerade ground state. The strong structured absorption and emission is thus assigned to the $^1\Sigma_u^+$ ($^1S + {}^1P$) ↔ $^1\Sigma_g^+$ ($^1S + {}^1S$) transition, in accord with other studies.[1,5,7-9] Additional support comes from the magnetic circular dichroism (MCD) spectrum to be published elsewhere[21] which gives a "B" term, thus ruling out the possibility of a degenerate excited state.

The lower energy structured absorption cannot be assigned

Table III. Summary of Gas-Phase and Matrix Constants

	$\bar{\nu}(0-0)$, cm^{-1}	ω_e, cm^{-1}	$\omega_e x_e$, cm^{-1}	D, cm^{-1}
		$^1\Sigma_u{}^+$		
Ar matrix	26 226	179	1.2	10 330– 12 888[c]
Gas phase[a]	26 139[b]	190.61	1.4	9311
		$^1\Sigma_g{}^+$		
Ar matrix		90.8	0.60	842–3400[c]
Gas phase[a]		51.12	1.64	399

[a] Reference 1. [b] Extrapolated from $v' \leftarrow 0$ series of ref 1. [c] Lower and upper limits; see text.

as unambiguously. Simple MO considerations and the more extensive theoretical work of Stevens and Krauss[18] give five possible states lower than the $^1\Sigma_u{}^+$ state. These include the $^1\Pi_g$ state mentioned above and the four triplet states derived from $^1S + {}^3P$ atomic limits. The triplet Mg_2 assignments can be ruled out as the observed band at 444 nm lies higher in energy than the $^3P \leftrightarrow {}^1S$ atomic transition (457.1 nm in the gas phase[22] and 480.1 nm emission in solid argon). Since the excited states are more strongly bound than the ground state, triplet molecular absorptions must appear lower in energy than the corresponding atomic transition. The most reasonable assignment for the weak band is to the formally forbidden $^1\Pi_g \leftarrow {}^1\Sigma_g{}^+$ transition of Mg_2. Symmetry-based selection rules are often weakened in a solid host owing to local matrix asymmetry. In addition, the vibrational spacings for the $^1\Pi_g$ state are expected to be higher than intervals for the $^1\Sigma_u{}^+$ state, based on calculated r_e values for these two states.[18] The higher observed vibrational spacings for the 444-nm absorption support this assignment.

Matrix Effects. Comparison of the matrix and gas-phase data allows qualitative evaluation of the effect of the matrix environment. The relevant constants are collected in Table III where they can be compared. The most striking difference occurs in the ground state constants, ω_e'', $\omega_e x_e''$, and D_e''. The fundamental vibrational frequency is almost twice as large and the anharmonicity is much less in the matrix as compared to the gas. Furthermore, the depth of the ground-state potential well is more than doubled from the gas-phase value and is shifted to shorter internuclear distance as described below. These differences reflect a matrix cage effect[23] which can impose a barrier to dissociation; i.e., a maximum is added to the potential curve. As a result, D_e'' and ω_e'' would be increased and $\omega_e x_e''$ decreased from the gas-phase value, as is observed. It is expected that such an effect would be most prominent for the most weakly bound states, although it must have some effect in all cases. Thus the constants for the more strongly bound $^1\Sigma_u{}^+$ state are quite similar in both the matrix and gas phase. The same cage effect has also been observed for the van der Waals ground state of Ca_2 in rare gas matrices; however, the matrix to gas-phase difference, 81 cm^{-1} as compared to 65 cm^{-1}, is not as pronounced for Ca_2.[12,16,17]

If one assumes that the vibrational numbering is correct for both the gas and matrix spectra, a shift of only 87 cm^{-1} was observed for the matrix 0–0 band compared to the extrapolated gas-phase origin. This is interesting in view of the marked matrix effect on the ground-state potential function.

The change in the internuclear distance between the ground and excited states was determined from a Frank–Condon analysis in the following manner. Harmonic potential curves for the two states were generated from the spectroscopic constants. Frank–Condon factors were then calculated for a series of internuclear distances and compared to the observed intensities. The best fit appeared for an internuclear distance

change of 0.5 Å. This compares to 0.81 Å in the gas phase and is consistent with a matrix cage effect.

A final matrix effect concerns the vibrational relaxation of small molecules in solid rare gases. Gas-phase emission spectra usually include many progressions originating from excited vibrational levels of the excited state. In matrices, however, efficient vibrational quenching because of interaction with lattice phonon modes often results in only $v' = 0$ progressions in emission. Recently, though, a growing number of small molecules have been found to exhibit relatively slow ground- and excited-state vibrational relaxation (see the introduction to ref 16 and references cited therein). In particular, extensive unrelaxed emission has been observed from the calcium dimer[16] and attributed to an extremely short fluorescence lifetime. Hence, unrelaxed emission from the chemically similar Mg_2 molecule is of interest. Here, unrelaxed emission was observed from the $v' = 1$–6 levels implying that the relaxation rate must be on the order of, or slower than, the fluorescence decay rate. However, if vibrational relaxation were much slower, only unrelaxed progressions would be observed as opposed to both relaxed and unrelaxed seen here. It seems reasonable that the fluorescence lifetime for Mg_2 is similar to the 11 ± 1 ns lifetime measured[24] for Ca_2, and hence, vibrational relaxation requires on the order of tens of nanoseconds. Such extensive unrelaxed emission was not expected for Mg_2 since the excited state spacing is smaller than for most other molecules where hot emission has been observed. This results in a smaller energy gap between the solute vibrational energy and the local phonon frequencies which suggests more efficient quenching.

Conclusions

The magnesium dimer has been formed and trapped in a solid argon host at 10–12 K. The absorption and emission spectra have identified and characterized the strong $^1\Sigma_u{}^+ \leftarrow {}^1\Sigma_g{}^+$ transition and a weaker electronic transition. A relatively simple molecular orbital picture is sufficient to explain the bonding and spectroscopy of this very interesting molecule. Comparison with the gas-phase data has led to qualitative considerations of a matrix cage effect and of vibrational relaxation in rare gas matrices.

References and Notes

(1) W. J. Balfour and A. E. Douglas, *Can. J. Phys.*, **48**, 901 (1970).
(2) W. J. Balfour and R. F. Whitlock, *Can. J. Phys.*, **50**, 1648 (1972).
(3) W. J. Balfour and R. F. Whitlock, *Can J. Phys.*, **53**, 472 (1975).
(4) K. Sakurai and H. P. Broida, *J. Chem. Phys.*, **65**, 1138 (1976).
(5) H. Scheingraber and C. R. Vidal, *J. Chem. Phys.*, **66**, 3694 (1977).
(6) J. M. Brom Jr., W. D. Hewett, Jr., and W. Weltner, Jr., *J. Chem. Phys.*, **62**, 3122 (1975).
(7) L. Brewer and J. L-F. Wang, *J. Mol. Spectrosc.*, **40**, 95 (1971).
(8) L. B. Knight and M. A. Ebener, *J. Mol. Spectrosc.*, **61**, 412 (1976).
(9) J. C. Miller, B. S. Ault, and L. Andrews, *J. Chem. Phys.*, **67**, 2478 (1977).
(10) J. E. Francis, Jr., and S. E. Webber, *J. Chem. Phys.*, **56**, 5879 (1972).
(11) L. Andrews, W. Duley, and L. Brewer, *J. Mol. Spectrosc.*, in press.
(12) J. C. Miller and L. Andrews, *Chem. Phys. Lett.*, **50**, 315 (1977).
(13) B. S. Ault and L. Andrews, *J. Mol. Spectrosc.*, **65**, 102 (1977).
(14) W. Duley, *Proc. Phys. Soc., London*, **91**, 976 (1967).
(15) J. C. Miller and L. Andrews, to be published.
(16) J. C. Miller and L. Andrews, *J. Chem. Phys.*, **68**, 1701 (1978).
(17) J. C. Miller and L. Andrews, *J. Chem. Phys.*, to be published.
(18) W. J. Stevens and M. Krauss, *J. Chem. Phys.*, **67**, 1977 (1977).
(19) B. Meyer, "Low-Temperature Spectroscopy", American Elsevier, New York, N.Y., 1971, p 47.
(20) V. E. Bondybey and C. Fletcher, *J. Chem. Phys.*, **64**, 3615 (1976).
(21) R. L. Mowrey, E. Krausz, P. N. Schatz, J. C. Miller, and L. Andrews, to be published.
(22) C. E. Moore, "Atomic Energy Levels", *Natl Bur. Stand. (U.S.)*, *Circ.*, No. 467 (1952).
(23) B. Dellinger and M. Kasha, *Chem. Phys. Lett.*, **38**, 9 (1976).
(24) V. E. Bondybey, and C. Albiston, *J. Chem. Phys.*, in press.